ARO 29008.1-EL-SBI

AD-A249 651

FR-60208

(2)

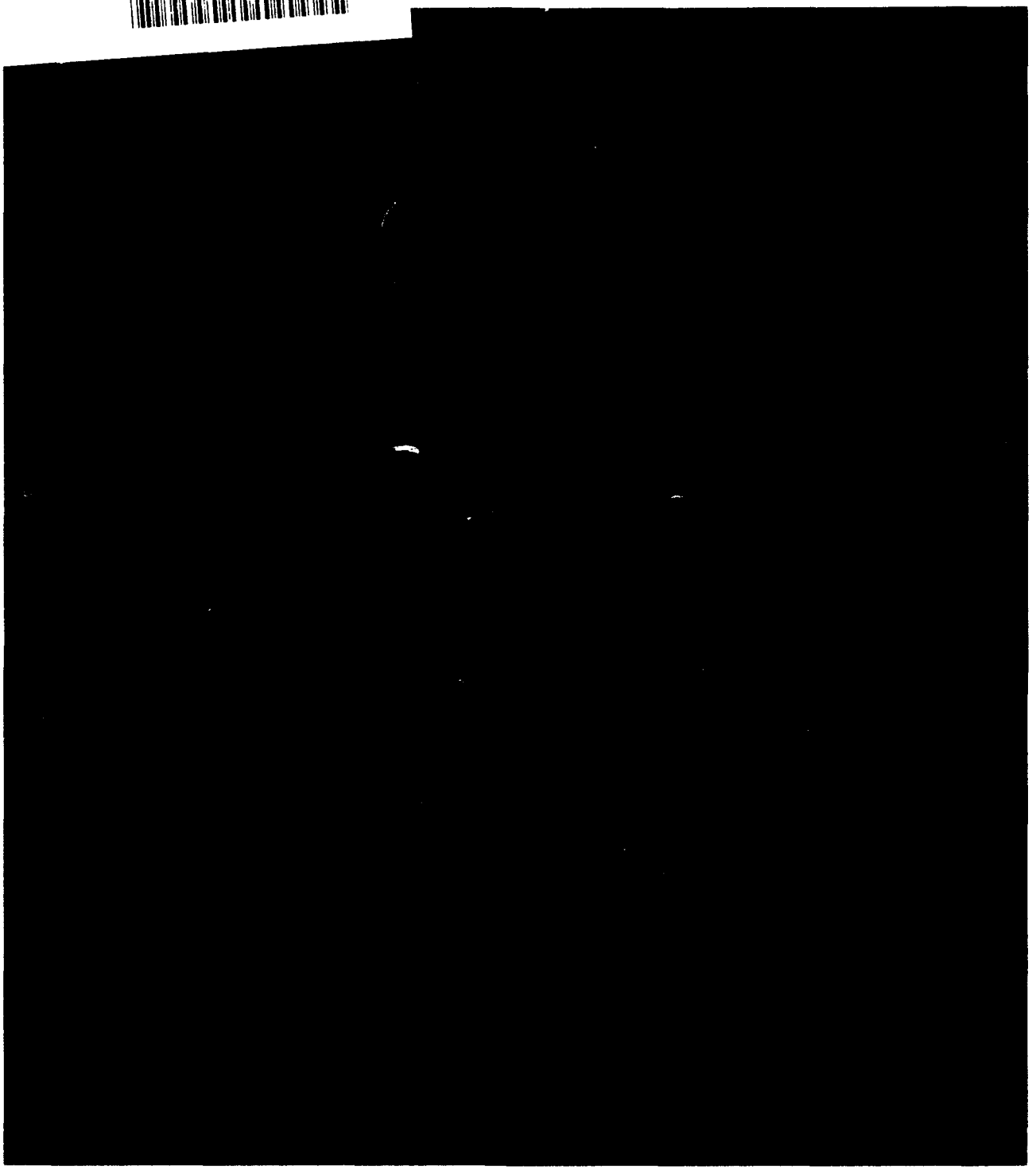

92-11111

spire

92 4 27 373

FR-60208

A Final Report for:

SiGe AND Si QUANTUM WIRES FOR EFFICIENT, ROOM TEMPERATURE, TUNABLE LUMINESCENCE

Contract Number DAAL03-91-C-0033

Submitted to:

U.S. ARMY RESEARCH OFFICE

P.O. Box 12211

Research Triangle Park, NC 27709-2211

SPIRE CORPORATION

One Patriots Park

Bedford, MA 01730-2396

REPORT DOCUMENTATION PAGE

Form Approved
OMB No. 0704-0188

1. AGENCY USE ONLY (Leave blank)	2. REPORT DATE	3. REPORT TYPE AND DATES COVERED
	2/3/92	Final Report - 7/1/91 - 12/31/91

4. TITLE AND SUBTITLE
SiGe and Si Quantum Wires for Efficient, Room Temperature, Tunable Luminescence

5. FUNDING NUMBERS
DAAL03-91-C-0033

6. AUTHOR(S)
Fereydoon Namavar, Sc.D., H. Paul Maruska, Ph.D., and Nader M. Kalkhoran

7. PERFORMING ORGANIZATION NAME(S) AND ADDRESS(ES)
Spire Corporation
One Patriots Park
Bedford, MA 01730-2396

8. PERFORMING ORGANIZATION REPORT NUMBER
FR-60208

9. SPONSORING/MONITORING AGENCY NAME(S) AND ADDRESS(ES)
U. S. Army Research Office
P. O. Box 12211
Research Triangle Park, NC 27709-2211

10. SPONSORING/MONITORING AGENCY REPORT NUMBER
ARO 29008.1-EL-SDI

11. SUPPLEMENTARY NOTES
The view, opinions and/or findings contained in this report are those of the author(s) and should not be construed as an official Department of the Army position, policy, or decision, unless so designated by other documentation.

12a. DISTRIBUTION/AVAILABILITY STATEMENT
Approved for public release; distribution unlimited.

12b. DISTRIBUTION CODE

13. ABSTRACT *(Maximum 200 words)*

A porous silicon visible light emitting diode has been developed. Porous silicon was prepared by electrochemically etching p-type silicon wafers in hydrofluoric acid solutions. Photoluminescence spectroscopy of these samples revealed intense light emission at wavelengths throughout the visible spectrum, as well as unusually strong emission at the band edge energy of bulk crystalline silicon. Emission intensities were comparable to those usually exhibited by high quality reference samples of GaAs. Thus quantum confinement of carriers in silicon nanostructures, created by the etch procedure, is indicated. Electroluminescence is observed from diode structures fabricated as heterojunctions between porous silicon and the transparent conductor indium-tin oxide, which serves as a window to allow light emission from the top surface of the device. Luminescence only occurs under forward electrical bias, while photovoltaic effects are seen under reverse bias. After the data are corrected for series resistance effects, the electroluminescent devices are shown to operate at junction biases of about 3-4 volts. A model based on minority carrier injection has been developed. Porous silicon light emitting diodes offer great promise for wafer scale integration of optical interconnects in high speed data processor applications, and to allow the construction of low cost flat panel displays, entirely in silicon.

14. SUBJECT TERMS
porous silicon, light-emitting diodes, visible electroluminescence, heterojunction diodes, quantum wires

15. NUMBER OF PAGES
25

16. PRICE CODE

17. SECURITY CLASSIFICATION OF REPORT	18. SECURITY CLASSIFICATION OF THIS PAGE	19. SECURITY CLASSIFICATION OF ABSTRACT	20. LIMITATION OF ABSTRACT
UNCLASSIFIED	UNCLASSIFIED	UNCLASSIFIED	UL

TABLE OF CONTENTS

LIST OF FIGURES

LIST OF FIGURES

SECTION 1
INTRODUCTION

Silicon is the basic building block for most integrated circuits, but present interconnects between high speed silicon microelectronic circuits in computer systems remain the exclusive domain of low speed, large area nests of copper wiring; furthermore, the associated displays which serve as the interface to human operators usually depend on bulky cathode ray tubes. We describe the formation entirely in silicon of visible light-emitting diodes (LED's) that promise to allow chip-to-chip, board-to-board, and system-to-human information transfer in an extremely efficient manner by optical means,[1,2] so that the silicon devices for emission, detection, and display of the information are monolithically integrated directly into the silicon wafers themselves. In the course of this Phase I effort, we have developed a technique for preparing silicon samples with nanostructural carrier confinement properties ("porous silicon") and, hence, have demonstrated photoluminescent emission throughout the visible spectrum, high intensity red light emission from samples with aqueous contacts, and surface-emitting visible light emitting diodes, all operating at room temperature. Silicon light-emitting devices and silicon photovoltaic detectors, embedded in each integrated circuit, would allow extremely rapid transfer of data within the processor. Since emission wavelengths throughout the visible spectrum have now been demonstrated with these porous silicon samples, it may be expected that, in the future, flat panel optical displays necessary for transferring the information from computer systems to human operators will be manifested entirely in silicon, as will chip-to-chip and board-to-board optical interconnects.

Although crystalline silicon has excellent properties for use as electronic amplifiers and switches ("transistors"), and junction diodes which feature minority carrier injection are readily demonstrated, its optoelectronic properties are severely compromised because the material possesses an indirect optical band gap. Basically, in order for an electron in the excited state (conduction band) of silicon to recombine into the ground state (valence band) while generating radiative emission, a third body, *viz.*, a phonon, must be involved, and such three-body processes have very low probability. Specifically, for any light-emitting diode, the radiative recombination rate is typically found to be proportional to the product $B(\Delta n)p$, where Δn is the concentration of injected minority carriers, p represents the majority carriers, and B is a material specific constant. For example, $B = 7.2 \times 10^{-10}$ cm^3/s for direct gap GaAs, but only 1.8×10^{-15} cm^3/s for the indirect gap in silicon.[3] Thus, although luminescence in the near infrared at 1.1 eV (1100 nm) can indeed be observed in standard silicon samples, it is extremely weak.[4] In fact, the external quantum efficiency of forward bias electroluminescence at 1100 nm in conventional diffused crystalline silicon np junctions is less than 10^{-4}%, basically the result of the indirect bandgap.[4] In contrast, the external quantum efficiency of direct bandgap GaAs light-emitting diodes exceeds 1%.[5] Consequently, many attempts are underway to graft compound semiconductor light-emitting diode and laser diode technology onto the silicon VLSI processes. However, the most promising III-V light-emitting compounds, such as GaAs and AlGaAs, are not readily deposited directly onto silicon substrates due to lattice and thermal expansion mismatches; these materials' incompatibility problems generally degrade the performance of any III-V compound light-emitting devices grown onto silicon. Another approach involves fastening GaAs-type devices onto the surface of the silicon wafer, either with solder or with glue: this is a costly, time consuming, labor intensive process. Undoubtedly, if a process could be developed

that allowed efficient light emission to be obtained directly from the surface of the silicon chip itself, then a simple, low-cost method would be available for implementing optical interconnects and flat panel optical displays, and all other processes presently being pursued would be superseded.

It has recently been reported that highly efficient, optically excited visible light emission (photoluminescence) is indeed possible from silicon[6] if the material is properly prepared in a microporous form, typically by electrochemical and/or chemical etching.[7] As a direct consequence of the etch procedure, such porous silicon samples are composed of a sponge-like network of channels which support a myriad of microscopic protuberances in the form of clusters located all over the internal surfaces of the pores. High magnification transmission electron microscopy (TEM) appears to confirm the presence of these basically one-dimensional structures, 10 nm or less in diameter.[8] Such nanostructures may be expected to exhibit quantum confinement effects, leading to a large increase in the effective energy gap: In fact, the absorption edge for such "wires" with roughly a 20 Å diameter was shown to be shifted to a wavelength of about 550 nm, which is in the yellow-green part of the visible spectrum.[9] Following the tasks of this Phase I program, we have fabricated samples of porous silicon on standard p-type crystalline silicon substrates by electrochemical means, tested their properties under optical excitation, and studied the effects of alloying with germanium. All of the program goals were met. Furthermore, we have proceeded beyond the statement of work and created np heterojunction porous silicon LED's that emit yellow light from the top surface, under forward junction biases of only a few volts.[10] This extended work initially proved to corroborate the results reported by Halimaoui *et al.*[11] who have formed liquid junction devices using aqueous HCl or KNO_3 solutions to inject electronic carriers into porous silicon films; however, both teams observed that the red light emission for these aqueous devices only lasted a few minutes, due to oxidation reactions. More recently, Richter *et al.*[12] describe using gold contacts deposited on n-type porous silicon to achieve light emission at 650 nm, with either dc or ac excitation, at 200 volts applied bias. Bassous *et al.*[13] have formed n-Si/porous-Si/p-Si devices which exhibit visible electroluminescence at low voltages from the side of a mesa. We will describe the fabrication of np heterojunction LED's which appear to have superior properties in that they are surface emitters and remain stable indefinitely; we shall also present a tentative model for the electroluminescence based on the device operating characteristics.

SECTION 2
PHASE I TECHNICAL OBJECTIVES

The original goal of this program was to develop a process which could alter the properties of silicon-based materials to allow the demonstration of efficient, room temperature, tunable luminescence. For the Phase I effort, we proposed to produce quantum wire structures in these materials by electrochemical etching of both bulk Si substrates and certain epitaxial layers. Due to the possibility of quantum confinement effects in such nanostructures, we expected to find that the band structure of silicon might be altered to favor direct transitions and, hence, to find samples that would be capable of efficiently emitting light. The proposed work furthermore required the deposition of $Si_{1-x}Ge_x$ alloys and the fabrication of quantum wires in these samples, also, to allow tuning of the emission spectrum. This could be achieved by varying the Ge concentration in the alloy series to provide a critical parameter for bandgap engineering. Therefore, epitaxial $Si_{1-x}Ge_x$ alloys were to be grown on Si substrates by chemical vapor deposition (CVD), followed by electrochemical etching to create nanostructures on the surface regions. The spectra and intensities of the emitted luminescence for both the pure silicon and the alloy samples were to be evaluated.

The effort has proven to be extremely productive: very significantly, intense photoluminescence emission peaks throughout the visible and near IR spectral regions were demonstrated, and their properties were studied over the temperature range from 4 to 700 K. Photoluminescence excitation spectra were also determined, as was the dependence of photoluminescence intensity on excitation intensity. The addition of Ge was shown to cause a red shift in the emission wavelength. Thus all of the tasks from the Phase I research program were successfully completed.

Of major importance is the additional work that was performed which extended the results beyond the contracted tasks. We observed red electroluminescence for cells that were configured as liquid junctions and, even more important, entirely solid-state heterojunction visible light-emitting diodes have been demonstrated. The results from Spire have achieved nationwide media attention and have been reported in a number of magazines and newspapers, including the Wall Street Journal, the New York Times, Science, Lasers & Optronics, etc. Spire's work has contributed greatly to efforts to develop optical interconnects and flat panel displays from silicon materials.

SECTION 3
EXPERIMENTAL PROCEDURE

We have used an Applied Materials Model 1200 epitaxy reactor to grow films of $Si_{1-x}Ge_x$ onto (100) silicon substrates; the substrates were four-inch diameter, p-type, 0.4-0.6 Ω-cm resistivity wafers, and the gas sources were silane (SiH_4) and germanium tetrachloride ($GeCl_4$). The composition and thicknesses of the layers were studied with Rutherford backscattering spectroscopy (RBS). A RUMP code was used to fit the data.

Figure 1 shows the anodic etching system used for producing porous Si and $Si_{1-x}Ge_x$ samples. This system relies on a Keithley Model 225 current source, with the sample connected as the anode (+), and a foil of platinum as the cathode (-). The electrolyte, usually a 1:1 mixture of hydrofluoric acid (HF) and ethanol, is contained in a teflon vessel. The silicon wafers are held in a specially prepared jig which only exposed the front surface to the solution, allowing electrical contact from the back, isolated from any liquid. The silicon sample is carefully etched in the HF solution at sufficiently low current levels so that the electrochemical reaction is limited by the supply of positive electronic carriers (holes) to the surface, rather than the availability of chemical species in the solution. Current densities between 2 and 20 mA/cm^2 were found to be effective in the process. The porous silicon surfaces were produced from p-type silicon wafers with either (100) or (111) orientations, and resistivities ranging from 0.3 to 14 Ω-cm. Shifts in the emission to shorter wavelengths could be controlled for any sample, whether bulk Si or epitaxial $Si_{1-x}Ge_x$, by increasing the duration of the etch procedure, as well as by allowing the *samples to remain passively (no bias applied)* in the HF for periods of time after the anodic etching was terminated.

Photospectrometry measurements were performed using Spire's photoluminescence system, shown in Figure 2. Excitation is created with a Coherent Model INNOVA-60 argon laser, set to emit a 5 mW unfocussed beam at 488 nm. The emission was dispersed with a SPEX Model 1702/04 grating monochromator and detected with a photomultiplier. An EG&G Model 5207 lock-in amplifier interfaced to a Hewlett-Packard model 86B computer served to collect the data. A cryogenic dewar was used for measurements at various temperatures down to liquid helium. High temperatures were achieved in an air environment, using a small thermostatically controlled hot stage capable of reaching 700 K.

We report a structure for a solid-state LED that represents work beyond the contracted tasks. Our device consists of a heterojunction between an electrochemically etched "porous" silicon sample and a transparent conducting oxide, *e.g.*, indium tin oxide (ITO) (see Figure 3). The deposition of an optically transparent n-type semiconductor onto the exposed porous silicon surface is carried out by rf sputtering. The ITO sputtering target consisted of an alloy of 91% In_2O_3 and 9% SnO_2. The material for the electron emitter layer was chosen to be capable of injecting negatively charged minority carriers (electrons) into the excited states ("conduction band" states) of the silicon nanostructures, while holes are supplied from the substrate. ITO has a relatively low work function, ~4.35 eV, which compares favorably with the electron affinity of bulk crystalline silicon, 4.05 eV, for allowing injection of electrons into silicon under forward bias; of course, the electron affinity of porous silicon is unknown at this time, so we cannot estimate *a priori* if minority carrier injection will indeed be favored.

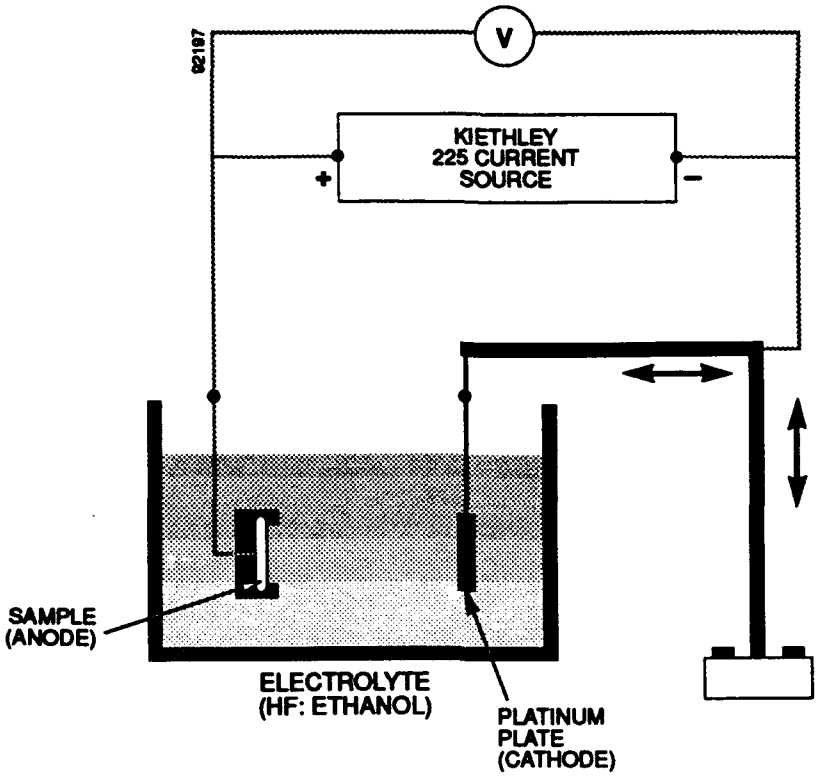

Figure 1 *Schematic diagram of the anodic etching system used at Spire for fabricating porous silicon samples.*

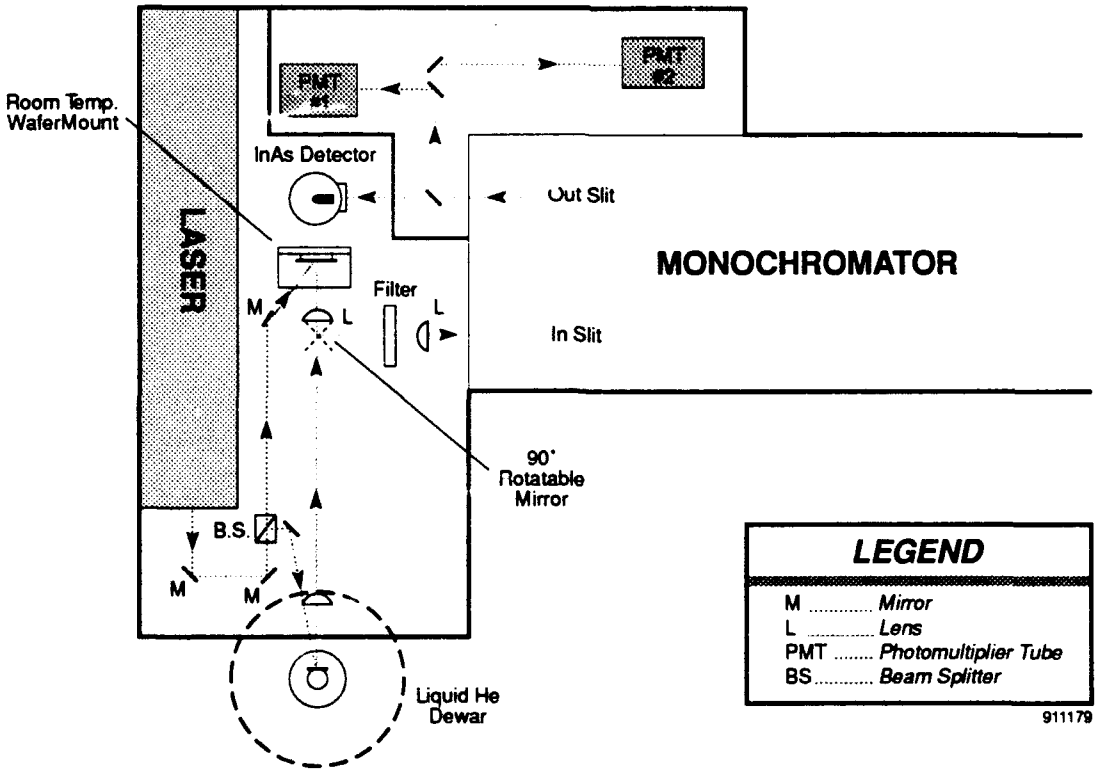

Figure 2 *Schematic diagram of Spire's photoluminescence system.*

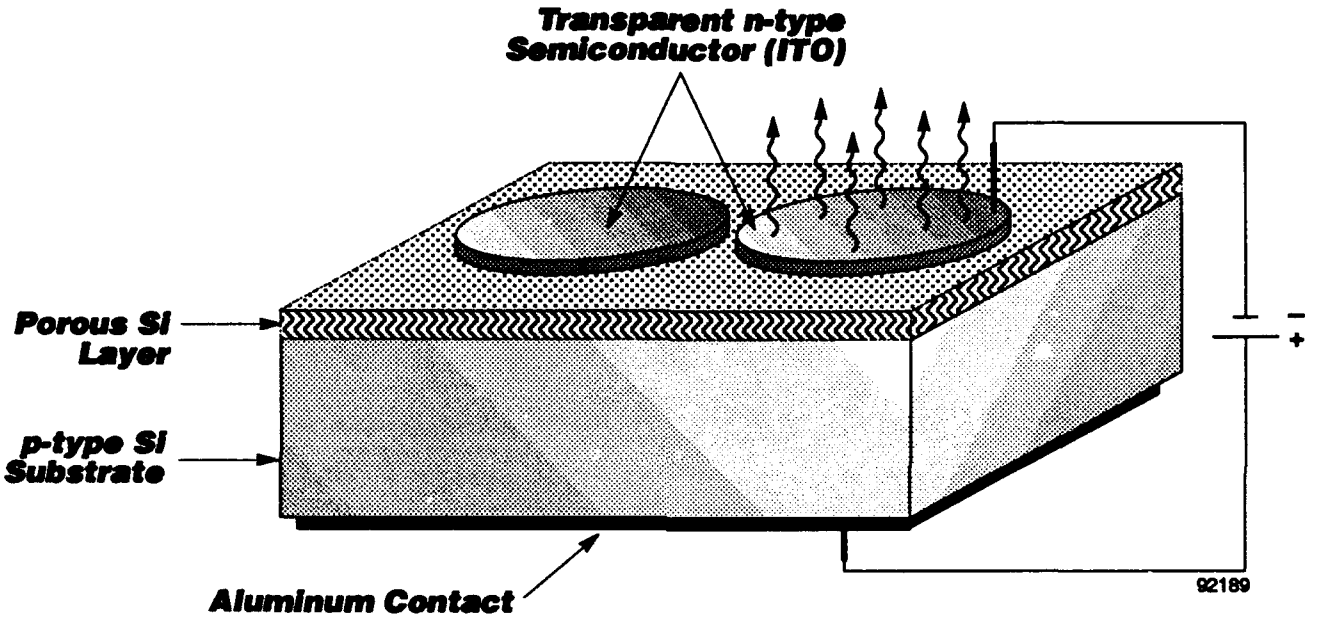

Figure 3 *Schematic of an np heterojunction surface-emitting porous silicon LED, capable of emitting light at visible wavelengths.*

SECTION 4
EXPERIMENTAL RESULTS

4.1 Materials Growth and Characterization

Using four-inch diameter p-type silicon substrates with (001) orientation, we grew a series of epitaxial films with varying concentrations of germanium. The composition and thickness of the grown layers was determined by Rutherford backscattering spectroscopy (RBS). The RBS data for sample 1022 is exhibited in Figure 4. Using a RUMP code to fit the data, we estimate that the layer of $Si_{1-x}Ge_x$ is about 1.7 μm thick, and has a germanium concentration x = 9.5%. Sample 1026 was prepared with a higher germanium concentration. A RUMP fit to the data is presented in Figure 5. This layer was about 1.8 μm thick and had a germanium concentration x = 19%. In all cases, the $Si_{1-x}Ge_x$ epitaxial layers appeared to be free of contaminants and to possess a uniform composition.

Clearly, the goal of producing high quality epitaxial films of $Si_{1-x}Ge_x$ has been successfully achieved.

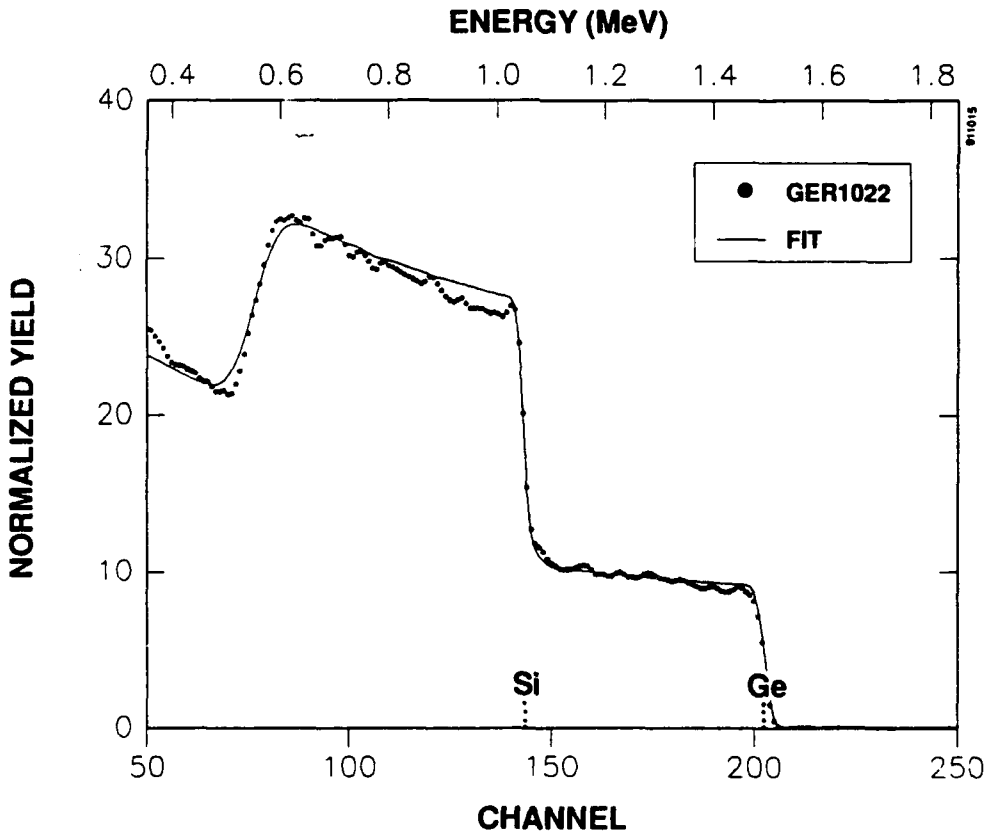

Figure 4 *RBS results for $Si_{1-x}Ge_x$ film on silicon, #1022: layer thickness is 1.7 μm, and the uniform Ge concentration is 9.5%.*

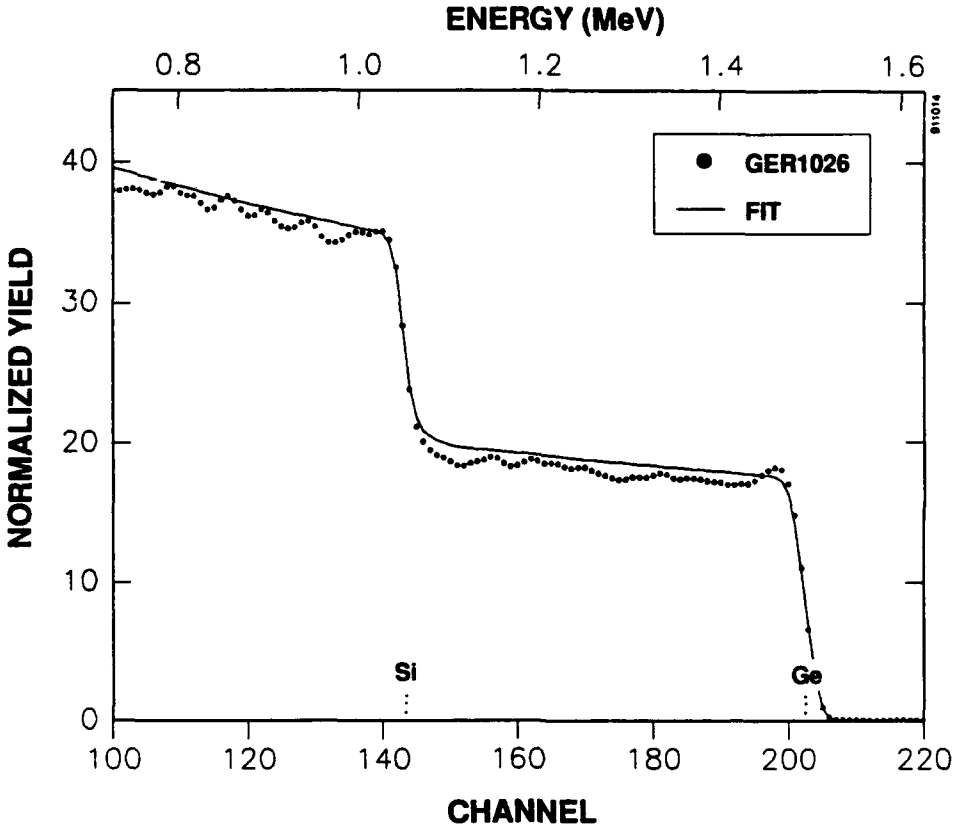

Figure 5 *RBS results for $Si_{1-x}Ge_x$ film on silicon, #1026: layer thickness is 1.8 μm, and the uniform Ge concentration is 19%.*

4.2 Fabrication of Quantum Wires

All of the wafers that were to be etched, whether bulk silicon substrates or substrates with grown epitaxial layers, were mounted in a specially designed jig. This jig had a circular opening at the front to allow the samples to make full contact with the etching solution; an o-ring protected the backs of the wafers from the liquid. The electrical contact was made to the back of each wafer. The jig was lowered into the solution of HF in ethanol, and current levels of 2 to 25 mA/cm^2 were supplied for varying periods of time. It could be seen that the surfaces of the samples developed a reddish-orange discoloration due to the etching. This color is due to the altered optical properties of the porous silicon films which were about 1 μm thick. When the surfaces of the etched wafers were scraped with a blade, a yellowish powder was obtained. Thus layers of porous Si and porous $Si_{1-x}Ge_x$ have been successfully prepared.

4.3 Optical Characterization of Porous Films

Extensive studies of the properties of the porous silicon and porous SiGe layers were performed. Figure 6 shows photoluminescence spectra of several porous silicon samples formed under different conditions of chemical etching, chosen to provide different wire diameters. Asymmetries in some curves are an artifact from an optical filter with cutoff characteristic at 520 nm, which was required to eliminate any photons emitted directly from the laser from entering the field of the detector. These red, orange, yellow, and green colors could be clearly

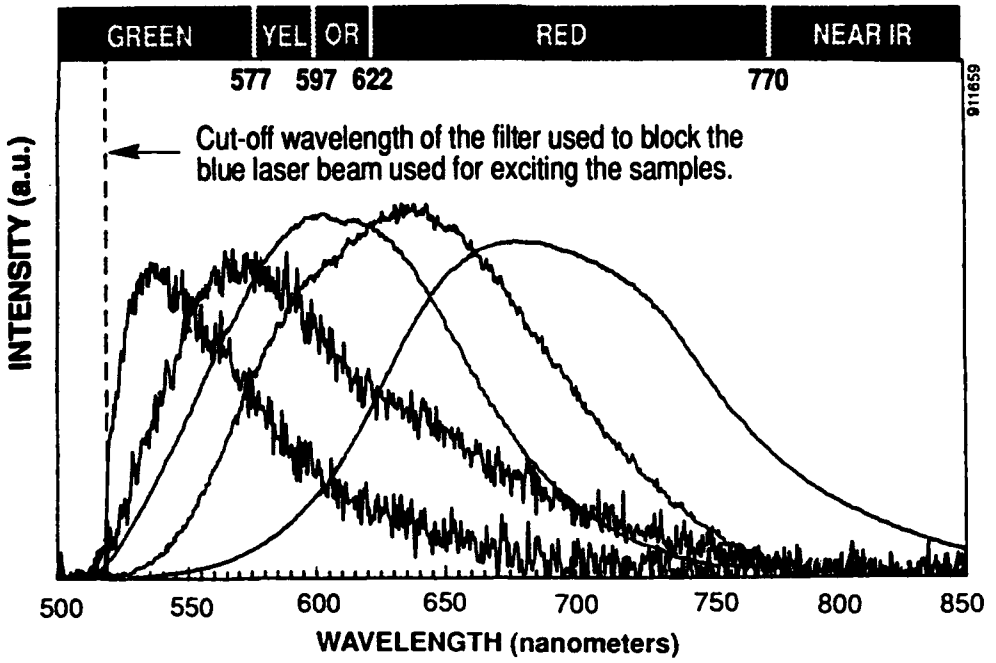

Figure 6 *Photoluminescence spectra of several porous silicon samples; excitation obtained with argon ion laser emitting at 488 nm.*

identified either on a series of samples prepared separately under different conditions, or spatially separated across the surface of a sample processed with graded properties. Longer etch periods always resulted in smaller nanostructures in the silicon, correlated with blue shifts in the emission wavelengths. The intensity of the photoluminescence was found to be essentially equal in intensity to that of a Spire reference sample of MOCVD-grown $Al_{0.30}Ga_{0.70}As$.

When alloys of silicon/germanium were prepared under conditions identical to those by which pure silicon samples were prepared, the peak wavelength of photoluminescence was always red-shifted, indicating that alloying with Ge tends to decrease the band gap of these structures. To our knowledge, we are the first laboratory to produce quantum wire structures with SiGe alloys successfully. The epitaxial layers were 1-2 μm thick, deposited by CVD at 1000°C. The structure and composition of a particularly promising sample with excellent surface properties were studied by RBS, and the data are shown in Figure 7. The sample contained about 6% Ge. This $Si_{0.94}Ge_{0.06}$ sample was anodically etched, as described above, for 90 minutes at a current level of 2-5 mA/cm^2. These are the same conditions used for bulk Si substrates. The photoluminescence results are shown in Figure 8, where the sample with 6% Ge is compared with pure Si. A red shift of the peak from 689 nm to 725 nm is clearly seen. This shift in the emission spectrum towards the infrared is extremely significant, because it supports the proposition that bandgap engineering can be utilized in the Si-Ge alloy series to tailor emission wavelengths.

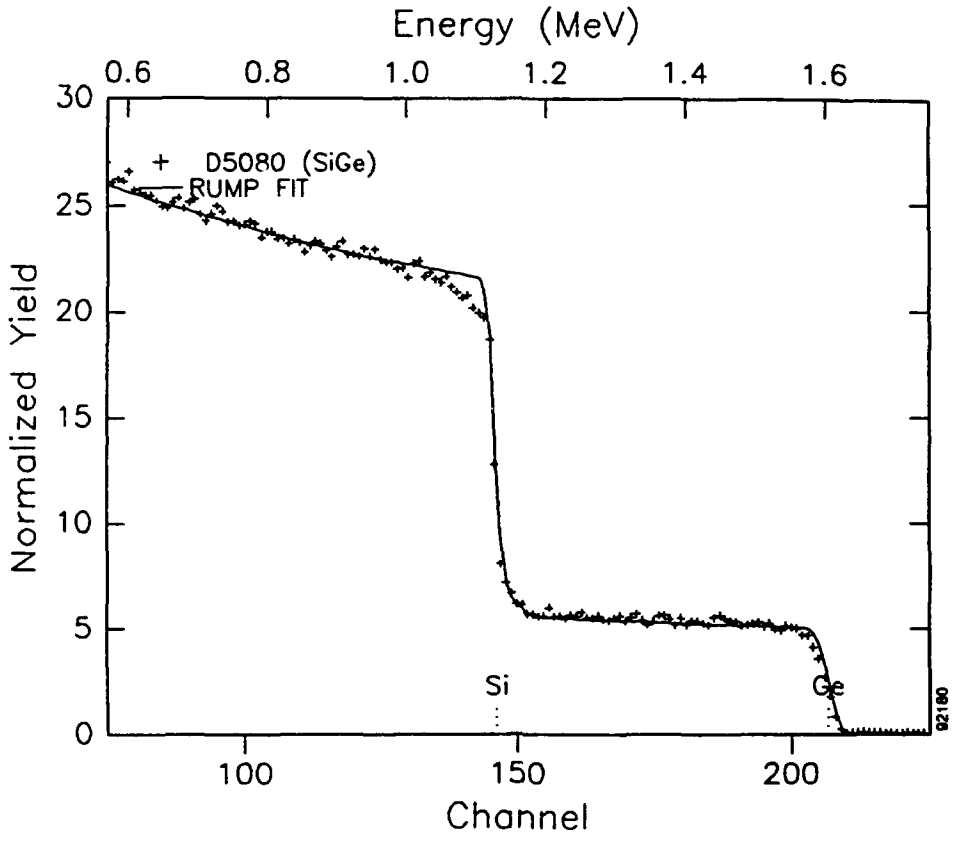

Figure 7 *RBS results for epitaxial $Si_{1-x}Ge_x$ layer grown by CVD, indicating Ge concentration of 6%.*

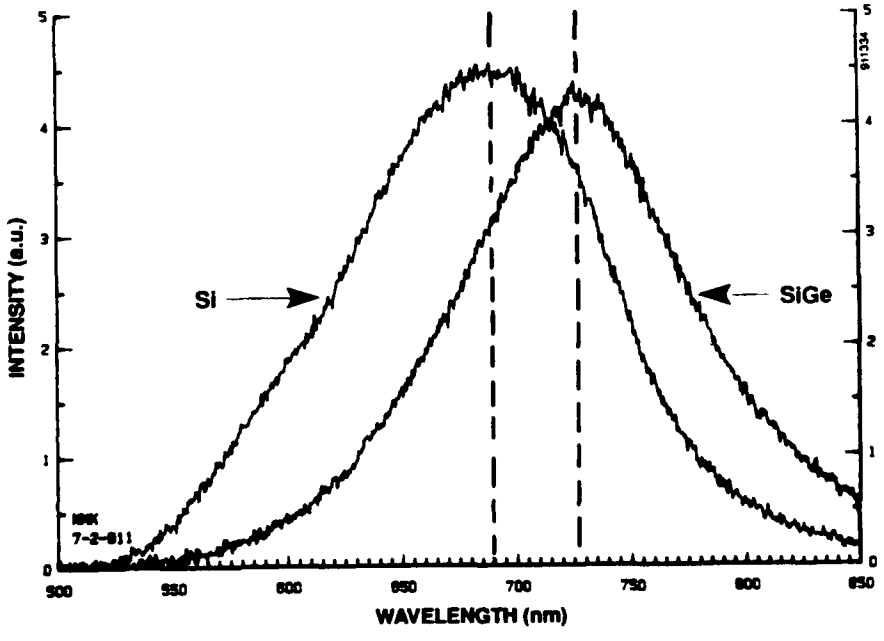

Figure 8 *Comparison of emission spectra of a porous silicon and a porous $Si_{.94}Ge_{.06}$ sample produced and tested under similar conditions.*

We studied the visible photoluminescence as a function of temperature (4-700 K), laser excitation wavelength (326 to 632 nm), and laser power (0.1 to 1000 mW). With increasing temperature, the photoluminescence peak decreased in intensity and shifted to longer wavelengths, both in air and in vacuum environments. Progressively lower photoluminescence intensities resulted from repeated heating and cooling cycles. The time dependence of the intensity of photoluminescence is shown in Figure 9; the rate of decrease in intensity lessened in each successive cycle. The intensity of photoluminescence increased with increases in the excitation power, but saturation was observed at high intensities, where heating was likely to occur. The photoluminescence peak red-shifted at the rate of -1.24 meV/K.

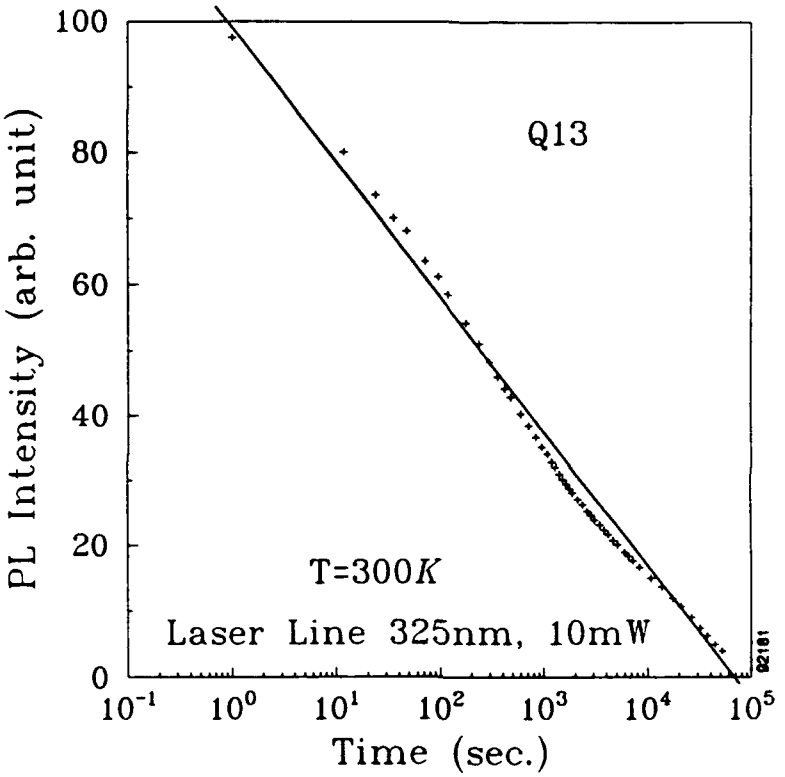

Figure 9 *Photoluminescence peak intensity at 690 nm as a function of time.*

Photoluminescence spectra for a porous silicon sample are shown in Figure 10 at several temperatures from 10 to 590 K. It is clear that the emission is red-shifted as the temperature is increased, while the emission intensity is seen to peak at about 150 K. The emission appeared to be totally quenched above about 600 K. The temperature dependencies of the intensity and the wavelength of the photoluminescence peak are shown in Figures 11 and 12, respectively. The photoluminescence intensity was strongly affected by the wavelength of the excitation, as shown in Figure 13. In fact, we estimate that when the porous silicon was illuminated by a laser emitting at 325 nm in the uv, the photoluminescence intensity was about 10 times as bright as when the sample was excited by 514.5 nm light. It appears that the photoluminescence is approaching a resonance in the uv, which might be the E_1 gap at 3.4 eV, or the direct gap at 4.2 eV for bulk silicon.

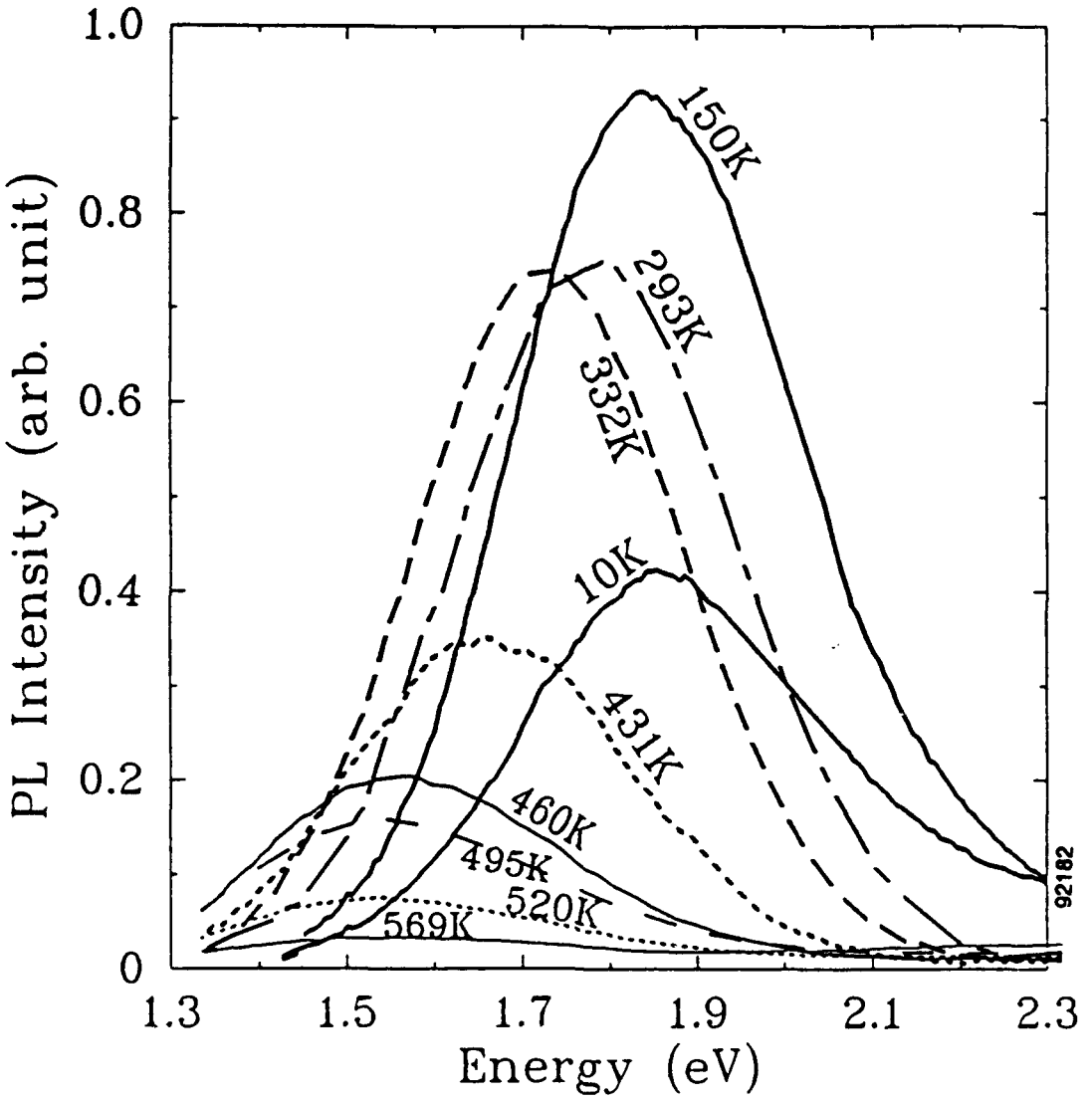

Figure 10 *Photoluminescence spectra as a function of temperature. Excitation with 10 mW at 458 nm.*

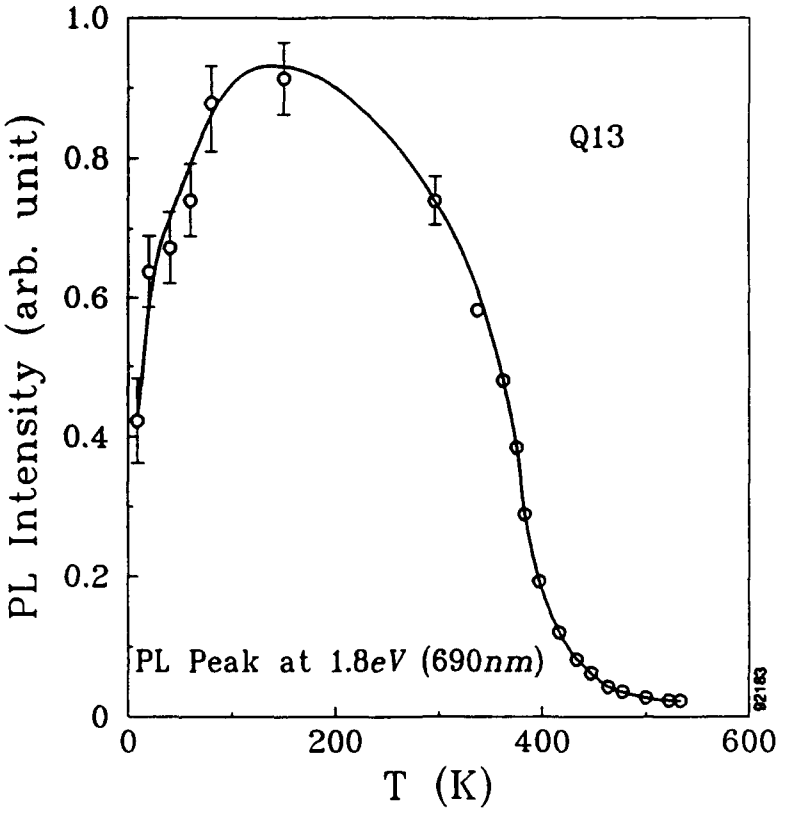

Figure 11 *Photoluminescence peak intensity as a function of temperature.*

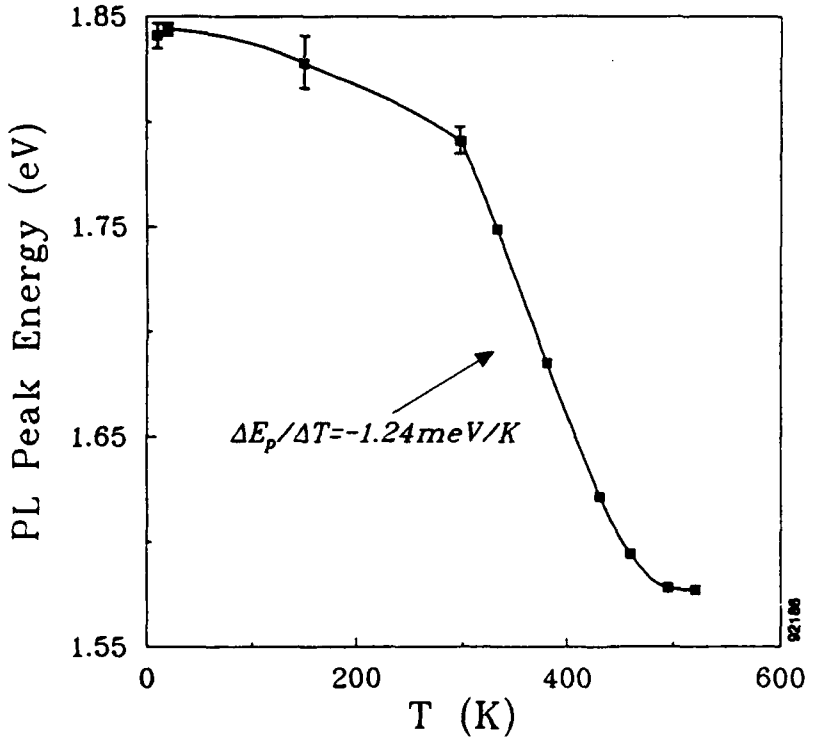

Figure 12 *Photoluminescence peak wavelength as a function of temperature.*

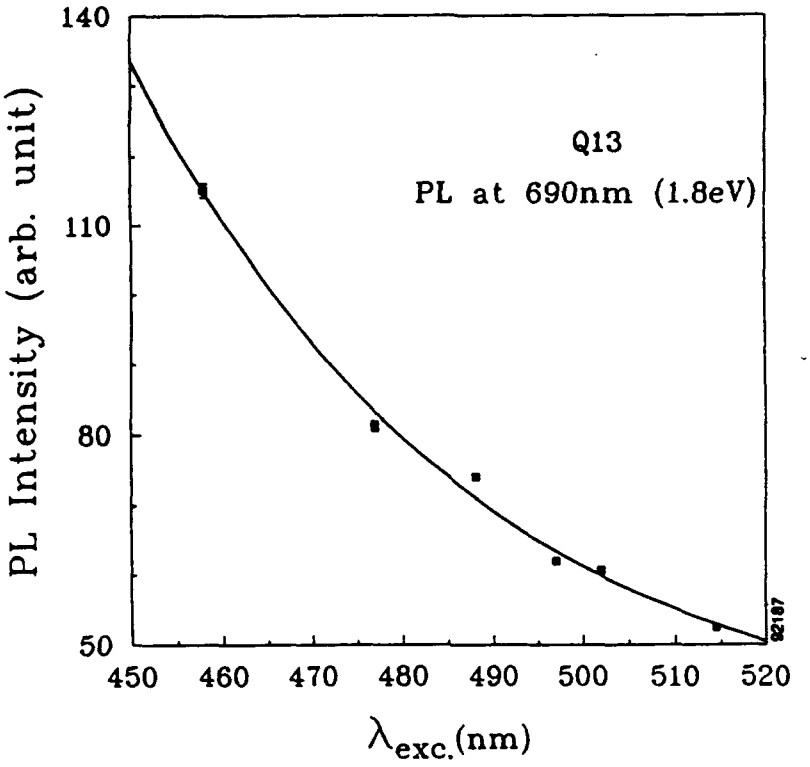

Figure 13 *Photoluminescence excitation spectrum.*

We report a remarkable increase in intensity of photoluminescence occurring at 1.10 μm at 300 K for our porous silicon samples, in the vicinity of the band gap of bulk crystalline silicon. This luminescence, which may be attributed to band-to-band recombination, was at least two orders of magnitude more intense than the emission from unetched silicon wafers. The intensity of the IR peak is estimated to be about 25% as great as the visible photoluminescence. The IR photoluminescence spectrum is shown as a function of temperature in Figure 14. At low temperature (4 K), the spectrum may be identified as intrinsic recombination including phonon emission from transitions at Δ (the conduction band minimum), which conserve momentum. The remarkable part of this figure is the strength of the phonon-assisted emission at room temperature; this feature may arise from the interface region between the porous silicon and the bulk silicon where defects are absent and only intrinsic recombination processes are possible.

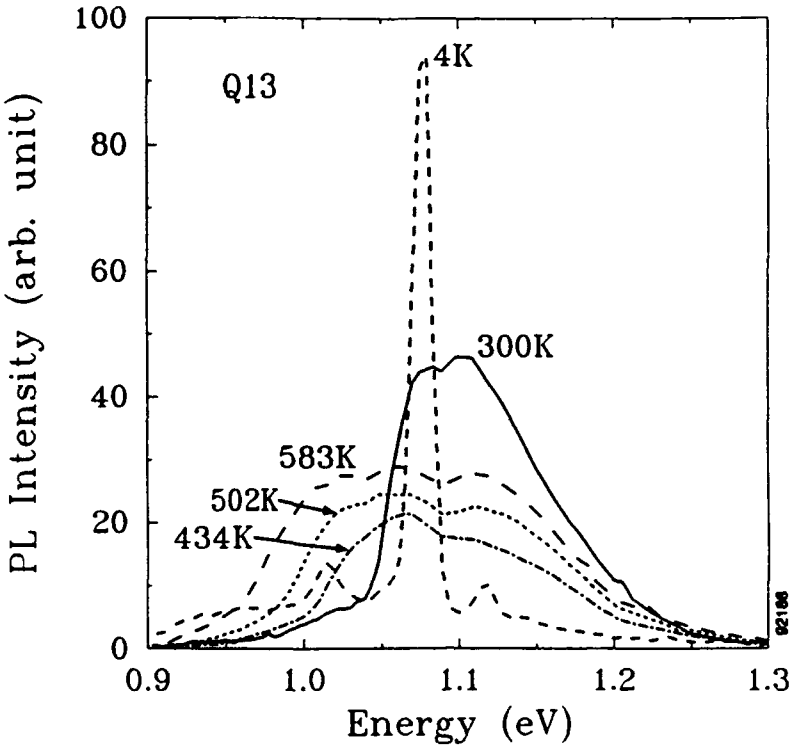

Figure 14 *Infrared photoluminescence spectrum from porous silicon, with emission near the band edge of bulk silicon.*

4.4 Summary of Contracted Tasks

All of the contracted tasks were successfully completed. High quality films of $Si_{1-x}Ge_x$ were deposited on silicon substrates and characterized. A system for producing nanostructures by electrochemical etching, both for bulk silicon wafers as well as epitaxial $Si_{1-x}Ge_x$, was developed. Photoluminescence from these samples was studied extensively. We obtained light emission both in the visible and in the infrared, and observed bandgap engineering possibilities when the silicon was alloyed with germanium. The photoluminescence intensity was found to be approximately equal to the intensities found with reference $Al_{0.30}Ga_{0.70}As$ samples, and colors ranging from red through green were manifested by varying the conditions of sample preparation.

Additional work which is of great significance has also been performed during our efforts, work that proceeds beyond the contracted tasks. We are pleased to present these results in the following sections.

4.5 Liquid Junction Electroluminescent Devices

When samples were held under anodic bias in aqueous NaCl solutions, broad areas of the surface were observed to emit visible light, appearing reddish to the eye, consistent with the report of Halimaoui *et al.*[11] The emission had a half-width on the order of 150 nm, with an intensity basically similar to the photoluminescence results. We have observed that the light emission in liquid junction cells ceased within a few minutes, most probably due to the growth of an electrically impervious oxide film on the surface of the porous silicon. However, it is encouraging to observe that the efficiency of minority carrier (electron) injection from the solution into the porous silicon appears to be sufficiently high so that electroluminescence intensity is comparable to photoluminescence. A typical spectrum of the liquid junction electroluminescence is shown in Figure 15.

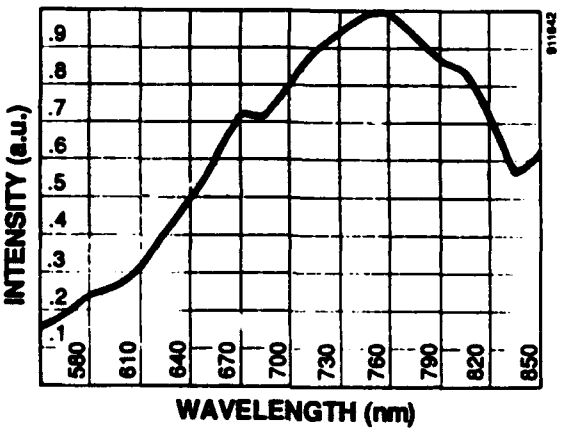

Figure 15 *Electroluminescence emission spectrum of liquid junction diode.*

4.6 Solid State Heterojunction Visible Light Emitting Diodes

We appear to be the first laboratory to have fabricated heterojunction porous silicon surface-emitting visible light-emitting diodes (LEDs). Under electrical bias, these devices were observed to emit visible light and appeared stable. These entirely solid state devices were fabricated in the form of heterojunctions between the transparent n-type semiconductor ITO and the p-type porous silicon, and showed strong rectifying behavior. We observed rapidly increasing current densities when the porous silicon was subjected to a positive bias and negligible current flow under reverse bias. Light emission was only observed under forward bias conditions, while photovoltaic effects, in response to incandescent illumination, were seen under reverse bias. No photocurrent was obtained at zero bias, possibly due to a photocurrent suppression mechanism.[14] Light emission intensities in the LED mode were measured with a Hamamatsu Type R889 photomultiplier, and this output was synchronized with the pulsed dc excitation of the LED. The dependence of the light intensity on the bias voltage is shown in Figure 16; it appears that the intensity depends linearly on applied voltage at large levels of bias. It will be shown below that, at high bias levels, the diode current depends linearly on applied voltage (series resistance limited), and, hence, in that range, the light intensity should depend linearly on injected current. A series of sharp cut-off low-pass optical filters were used for determining the emission spectrum of the device. Filters were placed sequentially between the sample and the detector, and each filter basically allowed transmission of the next 20 nm of wavelength, compared to the previous

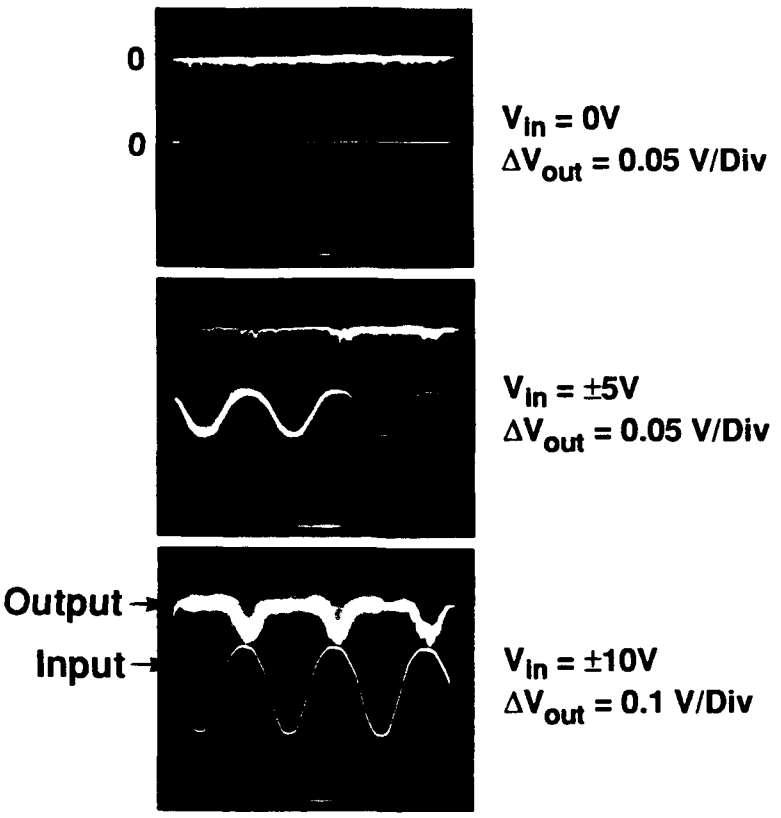

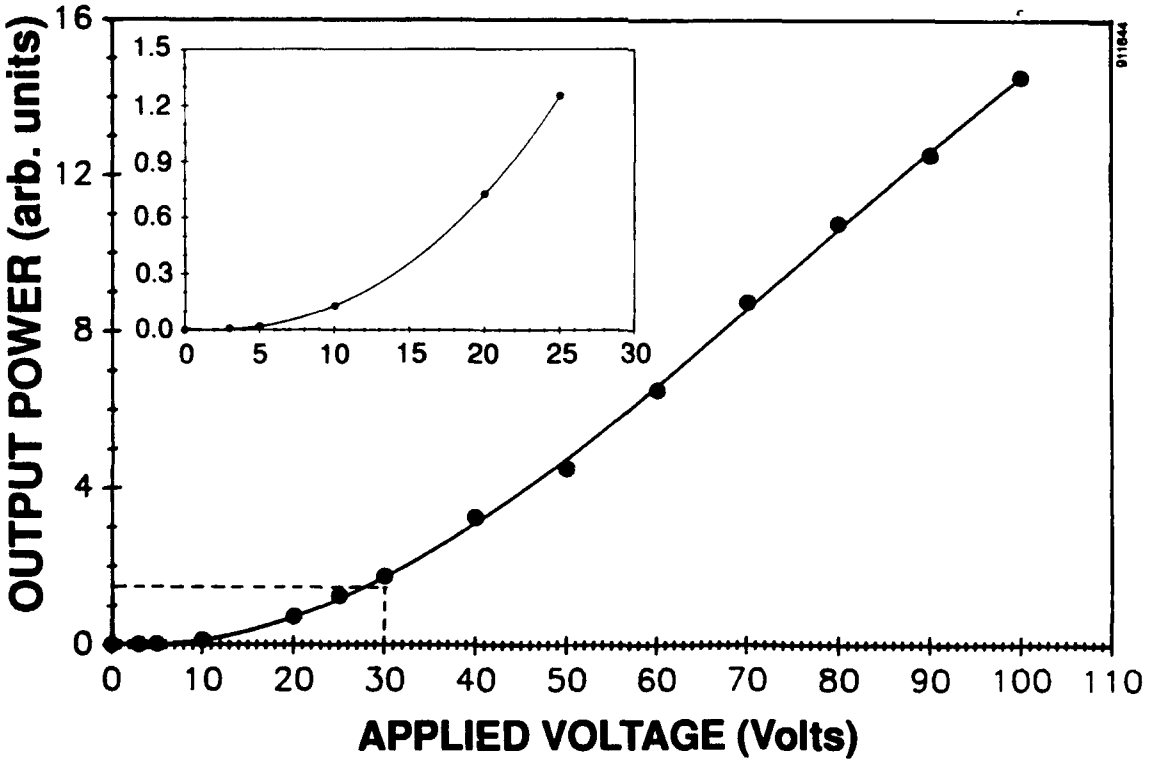

Figure 16 *np heterojunction LED: photomultiplier output level vs. bias applied to device.*

filter. The detector reading remained constant as filters starting with red transmission were exchanged, implying no emission of photons at such wavelengths, until a filter was inserted which allowed the band from 600 nm to 560 nm to pass, whereupon a large increase in signal was observed. No further increase in signal was found when filters allowing even shorter wavelengths to pass were used, and, furthermore, no signal intensity was measured when bandpass blue filters were in place. Thus we find that the emission appears to be in a relatively narrow (about 20 nm wide) band, centered at about 580 nm, as shown in Figure 17. The emission band appears to be much narrower than either the photoluminescence or liquid junction electroluminescence spectra, presumably because the smaller area of this solid-state device contacted a more uniform region of porous silicon than either optical or liquid junction excitation. We noted no decrease in the intensity of the light emission from a device after five hours of operation.

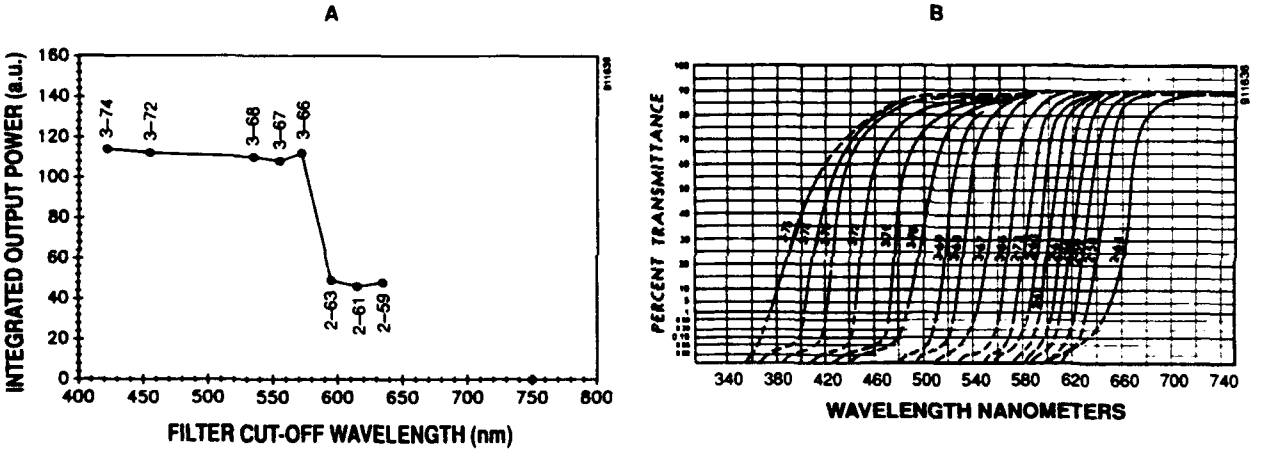

Figure 17 *a) Electroluminescence intensity for porous silicon LED resolved with a series of sharp cut-off low pass optical filters, indicating an emission peak at 580 nm; (b) Filter characteristics.*

Due to our method of preparation, we expect these devices to operate basically as heterojunction LEDs. The junction should occur between the wide bandgap, highly doped n-type emitter, and the p-type porous silicon base. Electroluminescence would result from injection of minority carrier electrons into the porous silicon material. (It is unlikely that holes could be injected into the n-type material due to a large potential barrier at the interface; no evidence of light emission in the ultraviolet has been observed). Indeed, we have observed strong rectifying properties for our junction diodes. Light emission was only observed in forward bias, *i.e.*, when the porous silicon is subjected to a positive applied voltage. The hypothetical "band diagram" is shown in Figure 18.

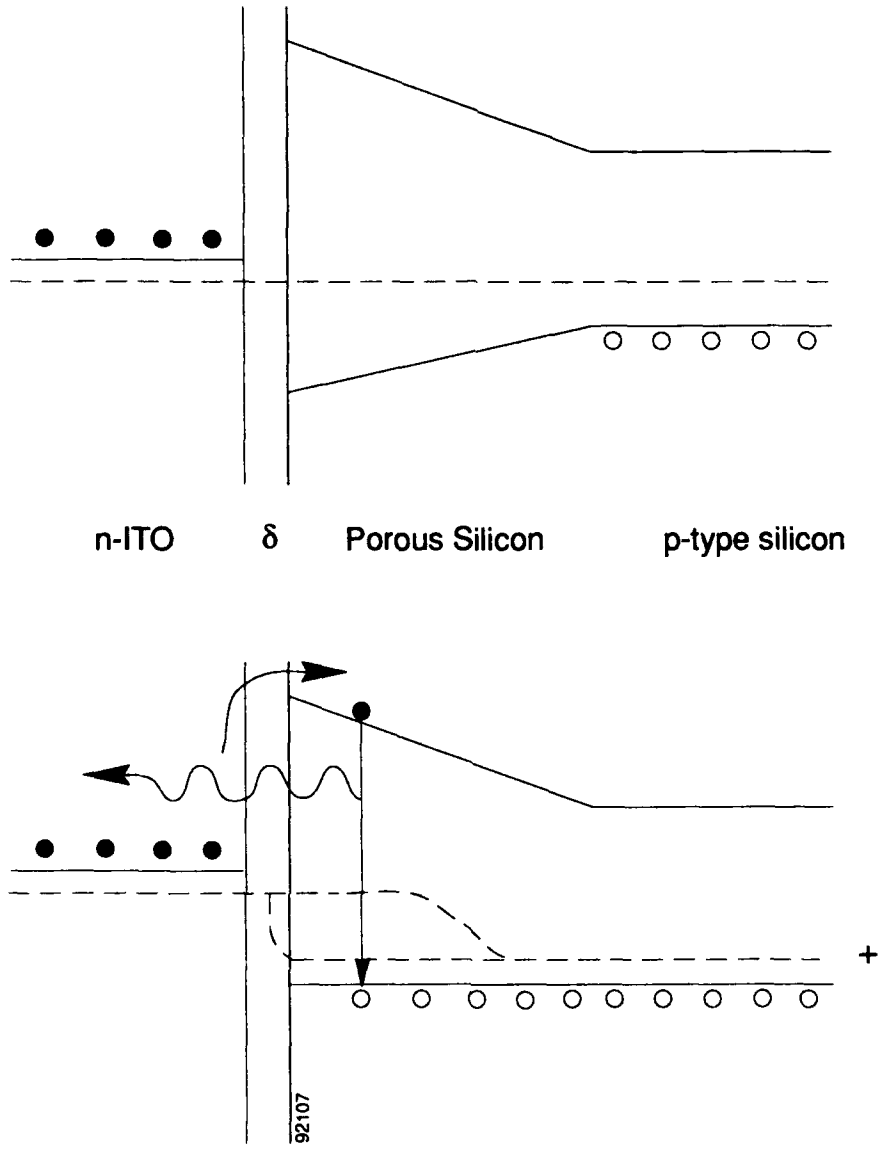

Figure 18 *Simplified hypothetical energy band diagram for a heterojunction between p-type crystalline silicon base, porous silicon emitter, and n-type transparent contact.*

The band diagram assumes that the properties of the porous silicon rods are essentially linearly graded in their electronic and optical properties. As one proceeds axially from the position in space where they are joined to macroscopic silicon regions, out to the ends or tips of these protuberances, no band structure "spikes" are present which would serve to trap carriers. We assume that the free carrier (hole) concentration in any rod is greatly reduced below bulk values, due to depletion. Forward (positive) bias applied to the base silicon will tend to flatten the potential of the valence band, allowing holes to enter the porous silicon rod region. Electrons can then be injected into the opposite end of the rod from a copious supply available from the n-type contact, across an n-p heterojunction. Electroluminescence is the result of recombination between the injected electrons and the majority-carrier holes.

Therefore, the electroluminescence that we observe is distinctly different from older reports of visible light emission from silicon under reverse bias.[15,16] Furthermore, the reverse-bias electroluminescence reported in the 1950's was very broad band, extending from the infrared into the ultraviolet, consistent with the proposed model of light emission from hot electrons in the conduction band under reverse bias. Our narrow emission band is consistent with minority carrier injection under forward bias. An example of a measured current-voltage characteristic is shown in Figure 19.

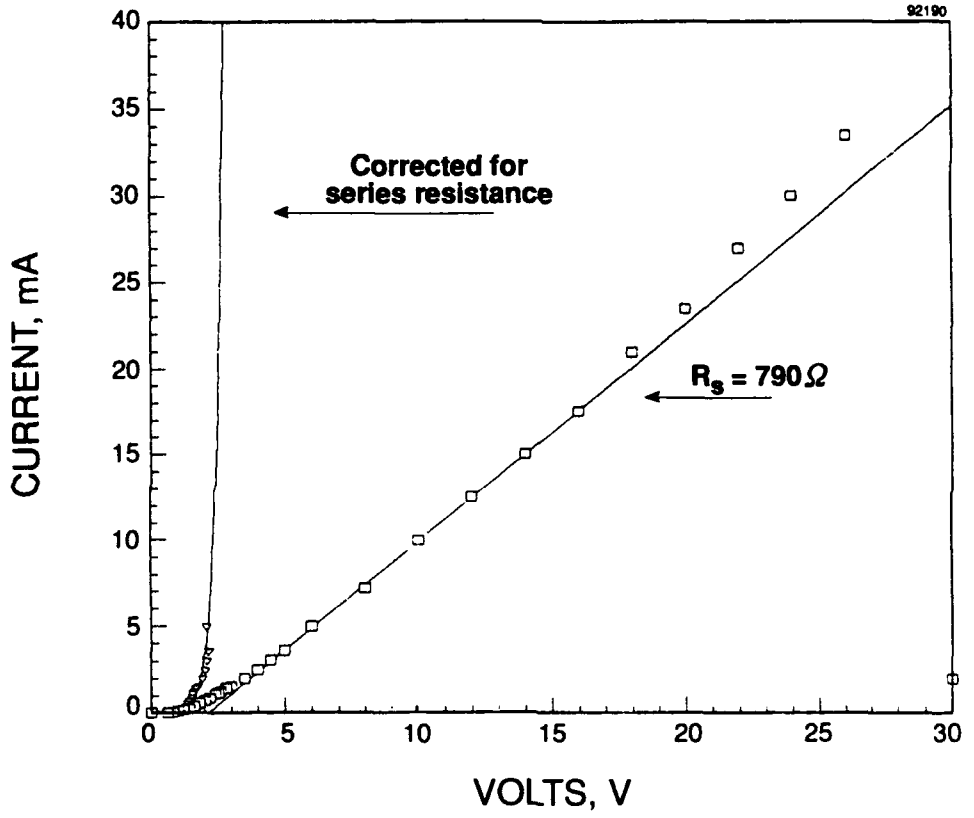

Figure 19 *Current-voltage characteristics of porous silicon heterojunction LED.*

The data indicate a relatively large value of series resistance R_s in the diodes. This resistance, calculated to be 790 Ω in this example, is due to non-optimized sample preparation procedures (particularly the ITO deposition), although alternatively it may reflect resistance to hole transport through the porous silicon. The resistance was determined by a linear regression analysis of the raw data. A significant fraction of the voltage applied to the diode is dropped across R_s, and hence we corrected the characteristic to obtain the dependence of the current on the junction voltage, also shown in Figure 19. An exponential regression analysis yielded the curve as shown, which gives an excellent fit to the data. The corrected data were then plotted in the standard log I vs. V format, as shown in Figure 20.

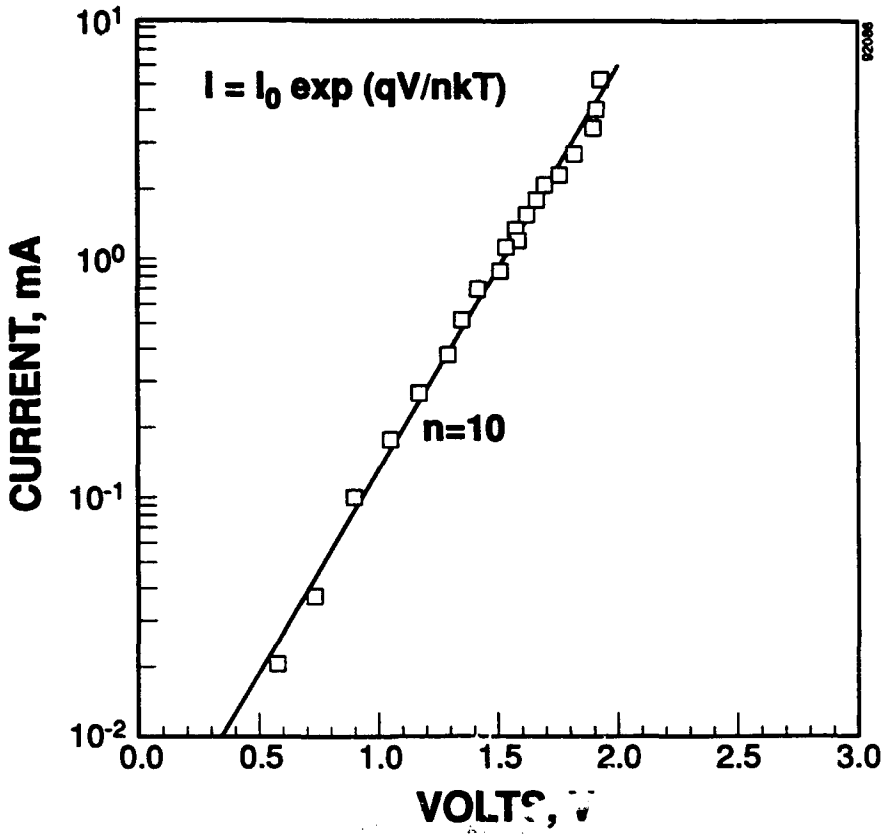

Figure 20 *Corrected current-voltage characteristic, indicating large diode ideality factor n.*

The corrected data give a good fit to the standard diode equation,

$$I=I_0\exp(qV/nkT) \qquad (1)$$

over almost three decades of current. This observation would be consistent with the model of a conventional n-p junction device. However, we observe that the calculated diode ideality factor n is 10, a rather high value. n>2 is often found with junction diodes formed between standard crystalline silicon and a transparent conducting oxide, such as ITO or SnO_2.[17] Maruska and coworkers,[18] based on the theory of Card and Rhoderick,[19] have explained diode ideality factors n>1 for tin-oxide/silicon diodes as follows. After accounting for any series resistance, it is found that the remainder of the applied voltage V is divided between the diffusion potential, V_D, across the semiconductor space charge region, and a potential V_i existing across an atomic scale interphase region of unknown composition with width δ, between the silicon and the indium tin oxide.[20] Changes in V_i are due to the charging of interface states which have a density D_s. This interphase region is expected to be composed of some compound of silicon and oxygen, with composition SiO_x (x<2), plus, in the case of porous silicon, other species such as H and F may also be present.

Therefore, applying these results to our present LEDs, the ideality factor n can be expressed as

$$\frac{1}{n} = \frac{\Delta V_D}{\Delta V} = 1 + \frac{dV_i}{dV} \tag{2}$$

From Gauss' Law applied across the porous silicon interface,

$$V_i = \frac{\delta}{\epsilon}(Q_{si} + Q_{ss}) \tag{3}$$

where Q_{si} is the charge stored in the interphase layer and Q_{ss} is the space charge in the semiconductor. Consequently, when a voltage V is applied, the change in V_i is given by,

$$\frac{dV_i}{dV} = \frac{\delta}{\epsilon}\left[\frac{dQ_{si}}{dV_D}\frac{dV_D}{dV} + \frac{dQ_{ss}}{dV_D}\frac{dV_D}{dV}\right] \tag{4}$$

which assumes that V_D is a function of both Q_{si} and Q_{ss}. Since $dQ_{ss}/dV_D = \epsilon/w$ and $dQ_{si}/dV_D = qD_s$, finally it is found that

$$n = 1 + \frac{\delta\epsilon_s}{w\epsilon_i} + \frac{\delta q D_s}{\epsilon_i} \tag{5}$$

where D_s is then the charge density ($cm^{-2}V^{-1}$) stored in the interphase layer at the semiconductor boundary, w is the width of the semiconductor space charge region, and ϵ_i, ϵ_s are the dielectric constants for the interphase and semiconductor regions, respectively. If n = 10, and using δ = 20Å, then D = 5.6 x $10^{13}/cm^2V$, which appears to be reasonable for the system in question. Clearly, improved devices will require reductions in the density of interface states, by chemically tailoring the surface of the porous silicon before heterojunction formation.

We may consider two other mechanisms which could govern the flow of current under forward bias, *viz.*, space charge injection and barrier tunneling. Since the porous silicon rods appear to be depleted, one might consider double (plasma) injection of holes and electrons, leading to a space charge. In this case, one expects to find that,

$$I = \frac{g}{V_0^{m-1}} V^m \tag{6}$$

a power law expression with m≥2. Using our porous silicon LED data, we obtain m = 4 - 5. Previously, Maruska *et al.*[21] explained m = 5.2 for n-i-p amorphous silicon diodes by invoking an exponential distribution of traps within the bandgap. Although this is reasonable for a disordered material such as α-Si, it does not appear to make physical sense for high quality crystalline silicon. Concerning current control by tunneling through a potential barrier at the n-i interface, Maruska and Stevenson[22] have proposed a model for current flow in GaN m-i-n diodes which can be described by,

$$I = gV\, e^{(\frac{V_0}{V})^{\frac{1}{2}}} \qquad (7)$$

the Fowler-Nordheim Equation. However, we could not fit our data on porous silicon LEDs to this formulation over any range of reciprocal voltage.

In light of the theory presented above, the energy band diagram shown in Figure 18 is reasonable. Basically, a forward bias will cause electrons to traverse the narrow interphase region (mechanism not presently known) to be injected into the conduction band of the porous silicon. Light emission near the band edge occurs through recombination with available holes. Considering that the n-type material is chosen to have a high mobile electron concentration, and the p-silicon was also highly doped with holes, then as long as majority carrier holes are not extracted from the porous silicon into the interphase region, high electroluminescence efficiencies would be expected. This competing mechanism appears to be limiting our efficiency at the present time. Work is underway to improve our understanding of the interface between the ITO and the porous silicon and to refine the current transport model.

SECTION 5
CONCLUSIONS AND RECOMMENDATIONS

Spire has developed a process for fabricating nanostructures in silicon and silicon/ germanium alloys, capable of exhibiting high intensity visible and infrared photoluminescence when excited by a blue or ultraviolet laser. Emission colors throughout the visible spectrum have been achieved basically by varying the conditions under which the samples are prepared. Samples were electrochemically etched in a solution of hydrofluoric acid in ethanol, at dc current levels of 2-25 mA/cm^2. The wavelength of emission could be red-shifted by alloying germanium with the silicon, grown as epitaxial layers onto crystalline silicon substrates.

Surface-emitting visible LEDs were fabricated as an extension of the program, beyond the contracted tasks. These heterojunction structures were created by sputtering thin films of indium tin oxide (ITO) onto the surfaces of electrochemically etched silicon wafers. Yellow electroluminescence, peaking at about 580 nm, was observed from these devices. Device characteristics were analyzed, and a tentative model based on minority carrier injection of electrons into the p-type porous silicon was proposed.

The surface of the porous silicon appears to be a critical factor in device performance. Unencapsulated samples suffered degradations in photoluminescence intensity over time, but the ITO/porous-silicon LED's appeared to be stable for indefinite periods. Much work needs to be done to identify the surface characteristics which play a critical role in allowing efficient radiative transitions in porous silicon. A further study of the properties of ITO in regard to light emitting properties of devices is warranted. Other materials may be found which possess superior properties to passivate the surface and to inject minority carriers while preventing the extraction of majority carriers. A more detailed examination of the greatly enhanced IR photoluminescence near the band edge of bulk silicon is a promising area for further study, since such emission wavelengths may find use coupled into SIMOX waveguides for intra-chip interconnects.

SECTION 6
REFERENCES

1. J.W. Goodman, F.I. Leonberger, S.Y. Kung, and R.A. Rathale, Proc. IEEE 72 850 (1984).
2. M.R. Feldman, S.C. Esener, C.C. Guest, and S.H. Lee, Appl. Opt. 27 1742 (1988).
3. Y.P. Varshni, Phys. Stat. Solidi 19 459 (1967).
4. W. Michaelis and M.H. Pilkuhn, Phys. Stat. Sol. 36 311 (1969).
5. H. Rupprecht, J.M. Woodall, K. Konnerth, and D.G. Pettit, Appl. Phys. Lett. 9 221 (1966).
6. L.T. Canham, Appl. Phys. Lett. 57 1046 (1990).
7. M.I.J. Beale, N.G. Chew, M.J. Uren, A.G. Cullis, and J.D. Benjamin, Appl. Phys. Lett., 46 86 (1985).
8. Y.H. Xie, W.L. Wilson, F.M. Ross, J.A. Muncha, and E.A. Fitzgerald, Mat. Res. Soc. Symp. Proc., Boston, MA, Dec. 2-6, 1991, to be published.
9. V. Lehmann and U. Goesele, Appl. Phys. Lett. 58 856 (1991).
10. N.M. Kalkhoran, F. Namavar, and H.P. Maruska, Mat. Res. Soc. Symp. Proc., Boston, MA, Dec. 2-6, 1991, to be published.
11. A. Halimaoui, C. Oules, G. Bomchil, A. Bsiesy, F. Gaspard, R. Herino, M. Ligeon, and F. Muller, Appl. Phys. Lett. 59 304 (1991).
12. Axel Richter, P. Steiner, F. Kozlowski, and W. Lang, IEEE Electron Device Lett. 12 691 (1991).
13. E. Bassous, M. Freeman, J.M. Halbout, S.S. Iyer, V.P. Kesan, P. Mungia, S.F. Pesarcik, and B.L. Williams, Mat. Res. Soc. Symp. Proc., Boston, Dec. 2-6, 1991, to be published.
14. R.L. Anderson, Appl. Phys. Lett. 27, 691 (1975).
15. A.G. Chynoweth and K.G. McKay, Phys. Rev. 102 369 (1956).
16. Roger Newman, Phys. Rev. 100 700 (1955).
17. Amal K. Ghosh, Charles Fishman, and Tom Feng, J. Appl. Phys. 50 3454 (1979).
18. H. Paul Maruska, Amal K. Ghosh, D.J. Eustace, and Tom Feng, J. Appl. Phys. 54 2489 (1983).
19. H.C. Card and E.H. Rhoderick, J. Phys. D: Appl. Phys. 4 1589 (1971).
20. S.J. Fonash, J. Appl. Phys. 46, 1286 (1975).
21. H.P. Maruska, T.D. Moustakas, and M.C. Hicks, Solar Cells 9 37 (1983).
22. H.P. Maruska and D.A. Stevenson, Solid State Electronics 17 1171 (1974).